

Marchant - Rankine's - Murzewski approach for modelling of the buckling resistance of welded I-section columns

Marian Giżejowski^{1*}, Marcin Gajewski¹ and Radosław Szczerba¹

¹Warsaw University of Technology, Faculty of Civil Engineering, Lecha Kaczyńskiego 16, 00-637 Warsaw, Poland

Abstract. This paper discusses different aspects of analytical and numerical modelling of the buckling resistance of welded I-section columns subjected to axial compression. The section considered is of class 1 that implies no local buckling affecting the column performance. The proposed analytical formulation of the buckling resistance is based on the so-called Marchant-Rankine's-Murzewski approach (M-R-M approach). The model proposed is of a 2D type and is a simplification of the 3D one that has recently been presented by the authors. The parameters of equivalent stress-strain model of the postwelding steel are calibrated in two stages of the best fit approximation procedure and with use of numerical results of the finite element simulation of the buckling resistance. In the first stage, the postyielding inelastic tangent stiffness parameter $\zeta_{E,eff}$ is evaluated with fixed value of the first yield parameter $\psi_{eff} = \psi_{com}$. A target of the second stage is to assign the best fit value of the first yield parameter ψ_{eff} and the imperfection factor n that allows for accounting the effect of geometric imperfections.

1 Introduction

Eurocode 3 design recommendations with regard to the buckling resistance of columns and beams are based on the Ayrton-Perry formulation [1] in which the combined effect of imperfections is modelled through the introduction of a slenderness dependent imperfection factor η of the following format:

$$\eta = \alpha(\bar{\lambda} - \bar{\lambda}_0) \quad (1)$$

in which α is the imperfection constant defining the buckling curve (represents globally the effect of imperfections on the buckling resistance as to the buckling dependency of real structural elements upon the section type, section wall dimensions, fabrication process and mode of buckling) and $\bar{\lambda}_0$ is a constant below which the buckling phenomenon does not affect the member behaviour.

A disadvantage of the approach such as that of Eurocode 3 [2] is that the buckling resistance cannot be evaluated as a function of the explicitly predefined parameters of material imperfections and geometric imperfections. One of the approaches that allows for the buckling resistance evaluation based on the independent treatment of imperfections is that of the Marchant-Rankine-Murzewski type (M-R-M approach) [3, 4]. In the 3D type of M-R-M approach presented by the authors in [5], two independent parameters \bar{e}_0 and ψ_{com} were introduced that describe in a dimensionless format the actual geometric imperfection profile and the actual postwelding residual stress pattern, respectively. It is based on the effective stress-strain diagram resulting

from either the equilibrium stress model (ES model) or the compatibility strain model (SC model). The latter model utilizes a virtual stub column test (VSC test) performed on a short length column with the actual residual stress pattern and conducted with use of the finite element simulation (FE simulation) and GMNIA type of the nonlinear incremental-iterative analysis [5]. In the conclusions summarizing the outcomes of conducted research it has been stated in [5] that the 3D M-R-M approach based on the VSC test leads to an unequal accuracy of the analytical model as to the buckling resistance evaluation with respect to the slenderness ratio.

The main aim of this paper is to simplify the formulation based on the 3D M-R-M approach by presenting its 2D version and applying the two stage best fit calibration procedure for the evaluation of the effective stress-strain diagram parameters instead of using the VSC test parameters from FE simulations. The numerical results of the column buckling resistance used hereafter for the calibration exercise have been obtained elsewhere for different parameters describing the column imperfections.

2 Buckling curve estimation based on the equivalent stress-strain diagram of postwelding steel

Let us consider the steel column of welded I-section of class 1, made of steel grade S355, the same as considered in [5]. The section dimensions are given in Fig. 1a. Fig. 1b presents a general residual stress pattern

* Corresponding author: m.gizejowski@il.pw.edu.pl

for such an I-section. The residual stress pattern is represented by a piecewise linear residual stress diagram with different ordinates of residual stresses in the tension and compression zones. Since the transition zone between the uniform residual stress blocks in tension and compression is rather small for welded sections, it is justified to adopt an approximate pattern consisting of rectangular residual stress blocks in tension and compression, without the transition zone. It yields $y_1=y_2$ and $z_1=z_2$ with different maximum stress ordinates in tension and compression. For common steel grades, the postwelding tensile residual stress $\sigma_{res,ten}=\psi_{ten}f_y$ reaches the steel strength (thus $\psi_{ten}=1$). Such an approximation of the residual stress pattern has been considered in [5] and maintained also hereafter.

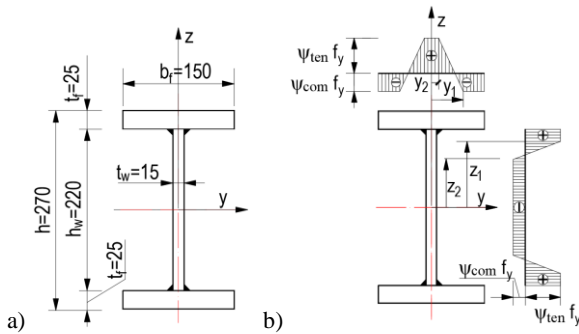


Fig. 1. Cross section, a) geometry, b) standard residual stress pattern.

The tension zone residual stress parameter ψ_{ten} is kept constant for different heat/cooling history so that only the compression zone residual stress parameter ψ_{com} might be considered as a variable. Discrete values from the range between zero (the residual stress free case) and 0.5 (the most unfavourable case for typical welded I-sections equivalent to those of rolled I-sections) are considered hereafter with an interval of 0.1.

2.1 SE model

The SE model assumes that the column is strain free with the equilibrated residual stresses within the section being of the same pattern for all the sections along the column length. The adopted equilibrated residual stress pattern produces therefore the section stress resultants of zero values. When the parent steel is modelled using the elastic-ideal-plastic diagram, the equivalent stress-strain diagram of postwelding steel becomes trilinear (for considered steel grade is given in Fig. 2).

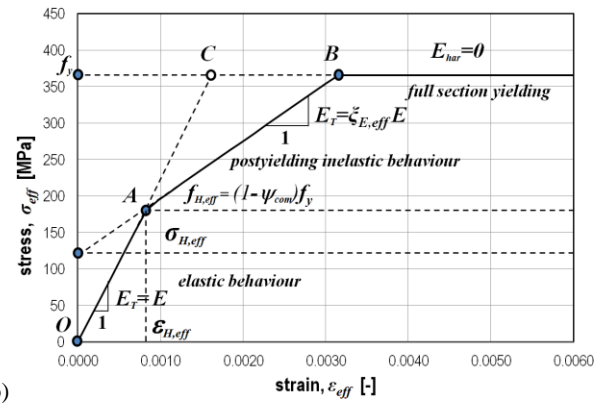
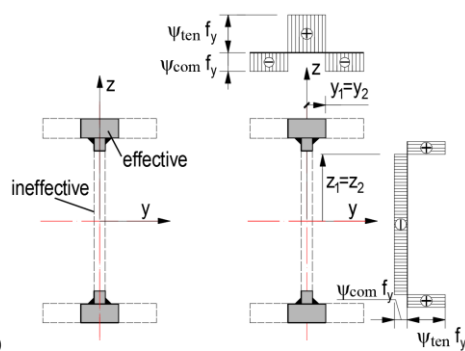


Fig. 2. Section properties affected by welding in the SE model, a) transformed cross section in the region AB, b) equivalent stress-strain diagram.

The initial line OA represents the column elastic behaviour up to the point at which the applied stress reaches the value $f_{H,eff}$ equal to $(1-\psi_{com})f_y$. At this point, the compression residual stress zones of the web and flanges yield. The original thickness t_i of yielded section i -wall (for the web $i=w$ and for the flanges $i=f$) might be represented by its effective (reduced) thickness according to the following equation:

$$t_{i,eff} = \frac{E_{har}}{E} t_i \quad (2)$$

For yielding without hardening ($E_{har}=0$), yielded zones become fully ineffective and the transformed section in the postyielding region consists only of the tension residual stress zones (Fig. 2a,b). The tangent modulus of the column effective stress-strain model may therefore be calculated from the following equation:

$$E_T I_z = E I_{z,eff} \quad (3)$$

in which

$$I_{z,eff} = I_{zw,eff} + I_{zf,eff}, \quad I_{zw,eff} = \frac{\alpha_w t_w^4}{6}, \quad I_{zf,eff} = \frac{\alpha_f t_f^4}{6} \quad (4)$$

The second line AB in Fig. 2b represents the section postyielding inelastic behavior after the first yield of residual stress compression zones of the cross section and the third, horizontal one beginning at B, represents the full section yielding (cross section is fully ineffective). For a given strain ϵ_{eff} , the stress σ_{eff} can be determined as a minimum of three variables where two of them are the functions of ϵ_{eff} and one is a constant:

$$\sigma_{eff} = \min(E \epsilon_{eff}, \sigma_{H,eff} + E_T \epsilon_{eff}, f_y) \quad (5)$$

in which the value of initial postwelding stress $\sigma_{H,eff}$ may be related to $f_{H,eff}$ and f_y as follows:

$$\sigma_{H,eff} = \left(1 - \frac{E_T}{E}\right) f_{H,eff} = \left(1 - \frac{E_T}{E}\right) (1 - \psi_{com}) f_y \quad (6)$$

2.2 SC model

The strain compatibility model requires either the real stub column test (RSC test) and real stub tie test (RST test) in the laboratory or their virtual representations (VSC test and VST test) obtained with use of numerical simulations. If a simple tensile test on a steel coupon is carried out, the stress-strain relationship will be a bilinear one and obtained from recording the data on a coupon measurement length L_0 . In numerical inelastic incremental analysis, the elastic-perfectly-plastic model of material based on a coupon test is usually replaced by its strain hardening counterpart in which a low value of the hardening modulus is adopted in the range of inelastic behaviour. The value of $E_{har}=E/1000$ is usually used (see Fig. 3a) and the relationship adopted is of the same form for tension and compression.

The stress-strain relationship is however different when a stub compression/tension test is performed. Let us consider a short I-section of the length L_0 such that in compression the buckling effect does not affect the specimen performance, therefore the stress-strain relationship obtained from the stub test, either RS test or VS test, will not be, due to residual stresses, of that from the coupon tensile test. Results of the VS test for the welded I-section and the considered standard postwelding residual stress pattern shown in Fig. 1a,b are presented in Fig. 3b. The curves corresponding to VSC test have also been derived in [5].

Let us consider in details one of the curves corresponding to the virtual compression test. It is shown in Fig. 4. The trilinear effective stress-strain curve obtained from this test is an approximation of the equilibrium path from the finite element simulation of the stub column test. First the best fit line A'B' is constructed together with that affected by hardening (B' is the intersection of both). The point C' is at the yield stress level and intersects with the hardening stiffness line. The initial part OA' of the equivalent $\sigma_{eff}-\varepsilon_{eff}$ relationship in the SC model is similar to that represented by OA line in the trilinear relationship for the SE model (Fig. 2). It has however to be noted that the point A' has a different stress level coordinate. The obtained equivalent $\sigma_{eff}-\varepsilon_{eff}$ is used for the determination of the buckling behaviour of the welded section steel column in the same way and that used in the SE model.

For a given strain ε_{eff} , the stress σ_{eff} can be determined as a minimum of three variables where all of them are the functions of ε_{eff} :

$$\sigma_{eff} = \min(E\varepsilon_{eff}, \sigma_{H,eff} + E_T\varepsilon_{eff}, \sigma_{har,eff} + E_{har}\varepsilon_{eff}) \quad (7)$$

in which the value of the stress $\sigma_{har,eff}$ may be related to f_y as follows:

$$\sigma_{har,eff} = \left(1 - \frac{E_{har}}{E}\right) f_y \quad (8)$$

as shown in Fig. 4b.

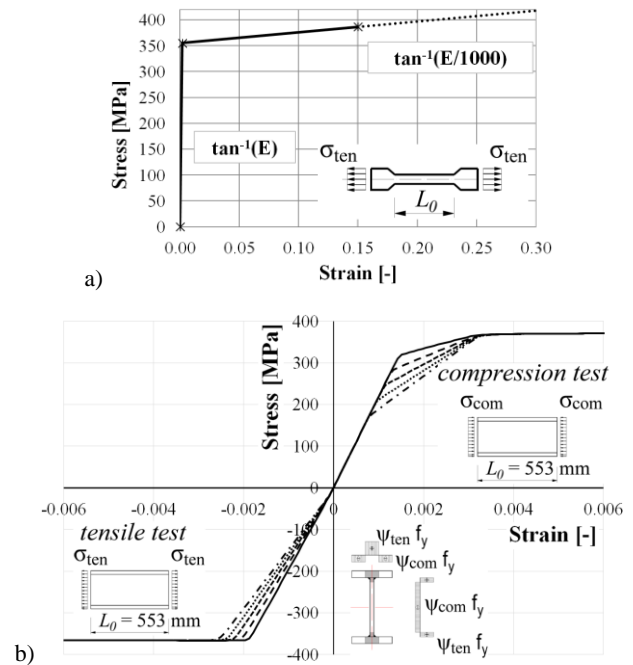


Fig. 3. a) coupon tensile test b) virtual stub column test for different values of ψ_{com} (compression and tensile tests).

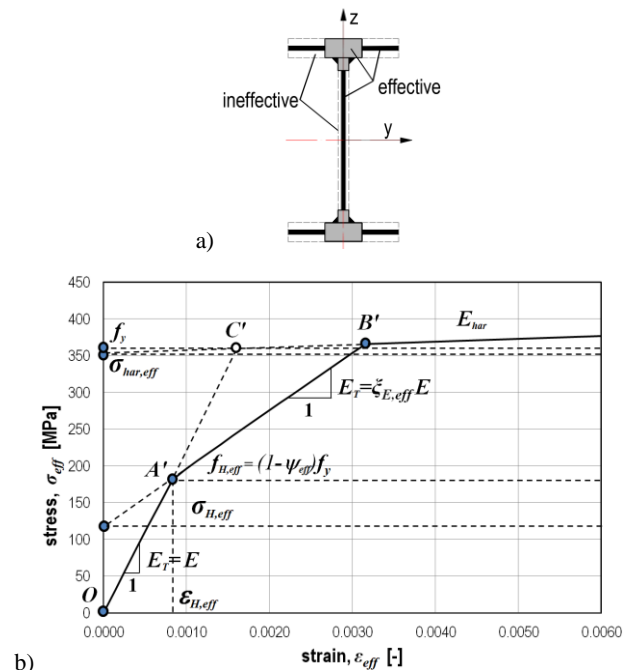


Fig. 4. I-section properties affected by welding in the numerical SC model, a) transformed cross section in the region A'B', b) equivalent stress-strain diagram.

2.3 Buckling curve approximation of perfect geometry postwelding column

When residual stresses are taken into account for steel columns being perfectly straight but of an arbitrarily length, two possible solutions are possible for assessing the buckling resistance in dimensionless coordinates $\chi_{z,res}$ and $\bar{\lambda}$:

LBIB: the lower bound inelastic bifurcation stress σ_b resulting from the tangent modulus theory of inelastic

buckling (Shanley's theory) for which the flexural buckling resistance about z-z axis affected by residual stresses is for $\sigma_b/f_y > 1-\psi_{eff}$ given by:

$$\chi_{z,res} = \frac{\sigma_b}{f_y} = \frac{\xi_{E,eff}}{\bar{\lambda}_z^2} \quad (9)$$

as shown in Fig. 5a,b by a blue solid line,

UBIB: the **u**pper **b**ound **i**nelastic **b**ifurcation stress σ_b resulting from the inelastic compression of the column without buckling up to the level of $\sigma_{H,eff}$ and then from buckling of the initially stressed column; thus the following relationship holds for $\sigma_b/f_y > 1-\psi_{eff}$:

$$\frac{\sigma_b}{f_y} = (1-\psi_{eff})(1-\xi_{E,eff}) + \frac{\xi_{E,eff}}{\bar{\lambda}_z^2} \quad (10)$$

as shown in Fig. 5a,b by a green solid line.

The above approximations need to be completed by the Euler curve for $\sigma_b/f_y < 1-\psi_{eff}$:

$$\frac{\sigma_b}{f_y} = \frac{1}{\bar{\lambda}_z^2} \quad (11)$$

that is shown in Fig. 5a,b by a red solid line.

The case $\psi_{com}=0.2$ is considered in Fig. 4 for which (see also Tab. 1):

- SE model parameters for **LBIB**: $\xi_{E,eff} = 0.005$ and for **UBIB**: $\xi_{E,eff} = 0.005$, and $\psi_{eff} = \psi_{com} = 0.2$,

- SC model parameters for **LBIB**: $\xi_{E,eff} = 0.209$ and for **UBIB**: $\xi_{E,eff} = 0.209$, and $\psi_{eff} = 0.167$.

The blue, green and red dashed lines are not in the range constituting upper and lower bounds of the buckling resistance.

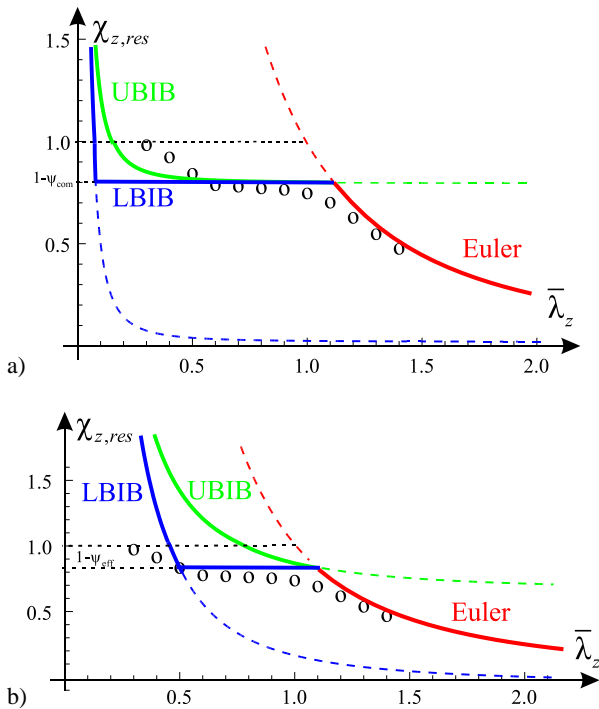


Fig. 5. Buckling curves assessment of welded perfectly straight columns, a) based on $\sigma_{eff}-\varepsilon_{eff}$ according to SE model, b) based on $\sigma_{eff}-\varepsilon_{eff}$ according to SC model.

In order to verify which model is closer to that from the incremental-iterative buckling analysis, LBIB or UBIB, a numerical GMNIA+ approach is adopted [6] and ABAQUS software used [7, 8]. The residual stress block is introduced through the option **Predefined Field, Mechanical, Stress* while the nonlinearity through the option **Nlgeom* and Riks algorithm for the evaluation of pre-limit branch, limit point and post-limit branch of the equilibrium path. In order to numerically trigger the buckling of perfectly straight column with the symmetric standard residual stress block about both axes, y-y and z-z, the infinitesimally small value of the amplitude is used for the column initially bowed according to the lowest buckling mode. The value of $e_0=L/10000$ is selected [5]. Numerical results in the slenderness range from 0.3 to 1.4 with an interval of 0.1 are given in Fig. 5 by blank circles.

The verification exercise shows clearly that neither SE model nor SC model is able to represent the buckling of perfectly straight column affected by postwelding residual stresses. A more accurate BF model is therefore proposed for the evaluation of $\xi_{E,eff}$ and ψ_{eff} parameters as it is explained in the following section.

2.4 BF model

The $\sigma_{eff}-\varepsilon_{eff}$ relationship parameters E_T and $\sigma_{H,eff}$ of the **best fit model** (BF model) are represented by their dimensionless equivalents $\xi_{E,eff}=E_T/E$ and $\xi_{H,eff}=\sigma_{H,eff}/f_y$ calibrated by the least square optimization with use of Mathematica function Non-Linear Model Fit. A two stage calibration procedure is proposed in which the calibration of $\xi_{E,eff}=E_T/E$ is firstly performed using the numerical results of $\chi_{z,res}$ and the fixed values of $\psi_{eff} = \psi_{com}$ giving $\xi_{H,eff} = (1-\xi_{E,eff})(1-\psi_{eff})$ according to Eqn. (6), and secondly – the calibration of ψ_{eff} parameters using the parameters $\xi_{E,eff}$ found in the first stage.

As a result of the above stated two stage calibration, the following linear functions are derived for the approximation of $\xi_{E,eff}$ and ψ_{eff} as a function of ψ_{com} :

$$\xi_{E,eff} = 0.001 + 0.105\psi_{com} \quad (12)$$

$$\psi_{eff} = 1.05\psi_{com} \quad (13)$$

The parameters used for the equivalent stress-strain relationships for three considered models, namely SE, SC and BF are listed in Table 1.

Table 1. Parameters describing the equivalent $\sigma - \varepsilon$ model.

Model	SE*)			SC**)	
	$\xi_{E,eff}$	$\xi_{H,eff}$	ψ_{eff}	$\xi_{E,eff}$	ψ_{eff}
0.1	0.001	0.133	0.066	0.012	0.11
0.2	0.005	0.209	0.167	0.022	0.21
0.3	0.013	0.273	0.267	0.033	0.32
0.4	0.025	0.327	0.368	0.043	0.43
0.5	0.038	0.375	0.470	0.054	0.53

*) The parameter $\psi_{eff} = \psi_{com}$, **) $\psi_{eff} = 1-\xi_{H,eff}/(1-\xi_{E,eff})$

3 Influence of postwelding residual stresses on flexural buckling resistance

In the following, the influence of postwelding residual stresses on the flexural buckling resistance is assessed. The results from FEM simulations are presented in Fig. 6 and compared to those of Eurocode 3 (in accordance with the EC3 specifications, the buckling curve "c" is designated to the analyzed cross-section). Five values of the ψ_{com} are taken into account, namely 0.1, 0.2, 0.3, 0.4 and 0.5. Two values of initial crookedness are considered: $e_0 = L/10000$ and $e_0 = L/750$ ($L/750$ is the amplitude at the manufacturing tolerance level). The results are presented in the following way:

- including postwelding residual stresses (with RS; labeled as blue circles for $e_0 = L/10000$ and black crosses for $e_0 = L/750$);
- excluding residual stresses (no RS; labeled as white circles for $e_0 = L/10000$ and red crosses for $e_0 = L/750$).

Observing the results, one can come to the conclusion that elements with the very small value of the geometric imperfection $e_0 = L/10000$ and without taking into account residual stresses could be treated as "perfect elements" (white circles). The inclusion of postwelding residual stresses led to the significant reduction of the flexural buckling resistance, but discrete values of the buckling resistance (blue circles) constitute the buckling curves of different shapes than those based on the EC3 recommendations.

The increase of the bow imperfection to the value of $e_0 = L/750$ led to the better match of FEM and EC 3 results. In case of the $\psi_{com} = 0.2$ (Fig. 6b, black crosses) the best fit of the FEM buckling resistances is obtained to those of the EC3 buckling curve "c".

Based on the above, it is important to emphasize that material and geometrical imperfections have to be considered individually in order to define the separate effect of material and geometrical imperfections on the column buckling strength.

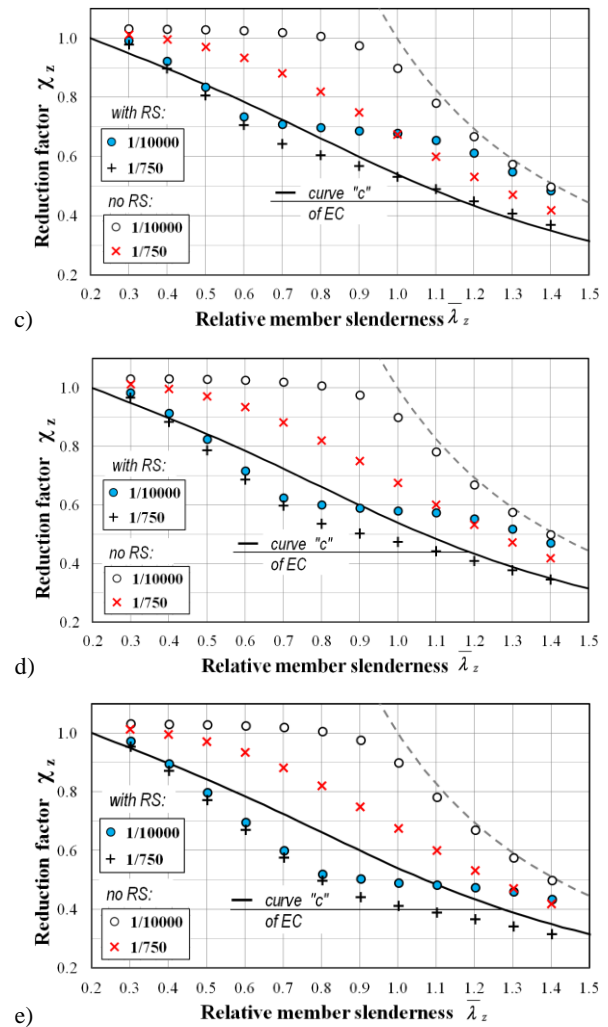
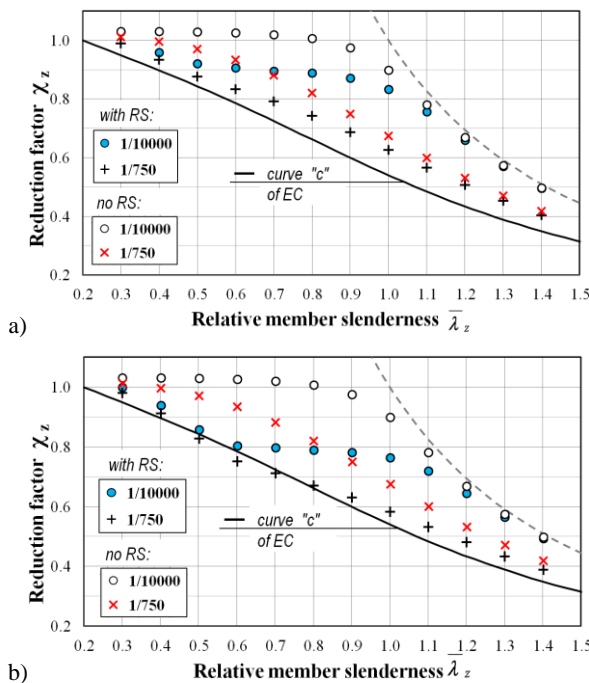


Fig. 6. Reduction factors χ_z from FEM simulations for steel grade S355, a) $\psi_{com}=0.1$, b) $\psi_{com}=0.2$, c) $\psi_{com}=0.3$, d) $\psi_{com}=0.4$, e) $\psi_{com}=0.5$

The aspects of FEM modelling and the problem of postwelding residual stress influence on the stability of steel members were also presented in [9-12]. An alternative method of assessing the load capacity of steel elements to this presented in the paper is the concept of equivalent geometric imperfections, which is in compliance with the so-called Eurocode's general method. FEM calculations with use of the concept of equivalent geometric imperfections were presented and widely discussed in [13-17]. The sensitivity and reliability analyzes of buckling resistance of steel members were presented in [18-20].

4 M-R-M buckling curve formulation based on BF model

The reference is made to the authors' paper [5] in which the M-R-M buckling curve formulation with three variables N_{cr} , $N_{cr,eff}$ and $N_{cr,har}$ based on the SC model parameters has been presented. It is simplified hereafter by reducing from three to two the number of the considered variable components, i.e. N_{cr} and $N_{cr,har}$ for $\psi_{com}=0$ or N_{cr} and $N_{cr,eff}$ for $\psi_{com} > 0$.



Thus, for perfect columns ($\psi_{com}=0$):

$$N_{b,nom} = \min(N_{cr}, N_{cr,har}) \quad (14)$$

and for columns with postwelding residual stresses ($0 < \psi_{com} \leq 0.5$)

$$N_{b,nom} = \min(N_{cr}, N_{cr,eff}) \quad (15)$$

The following notation is used: N_{cr} - Euler elastic critical force, $N_{cr,eff} = \sigma_{H,eff} A + \zeta_{E,eff} N_{cr}$ - critical load with residual stresses taken into account, $N_{cr,har} = (1 - \zeta_{E,har}) N_{pl} + \zeta_{E,har} N_{cr}$ - critical load referred to the hardening stiffness, $N_{pl} = Af_y$ and $\zeta_{E,har} = E_{har}/E$.

Using the conventional dimensionless coordinates used in Eurocode 3 [2], Eqns. (14) and (15) may be presented in a rearranged format:

$$\chi_z = \min[\bar{\lambda}_z^{-2}, (1 - \xi_E)(1 - \psi) + \xi_E \bar{\lambda}_z^{-2}] \quad (16)$$

where for $\psi_{com}=0$: $\xi_E = \zeta_{E,har}$ and $\psi=0$, and for $\psi_{com} > 0$: $\xi_E = \zeta_{E,eff}$ and $\psi = \psi_{eff}$.

The M-R-M approach leads therefore to a two dimensional Weibull minima distribution of the buckling resistance [4]. As a result, the following equation is obtained for the reduction factor χ_z of an imperfect column subjected to residual stresses and initial bow deformations:

$$(\chi_z)^n = \bar{\lambda}_z^{-2n} + [(1 - \xi_E)(1 - \psi) + \xi_E \bar{\lambda}_z^{-2}]^n \quad (17)$$

in which n is the imperfection factor to be best fitted to results of FEM simulations.

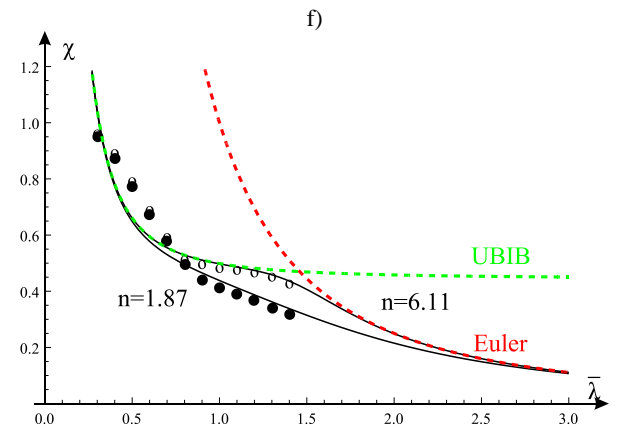
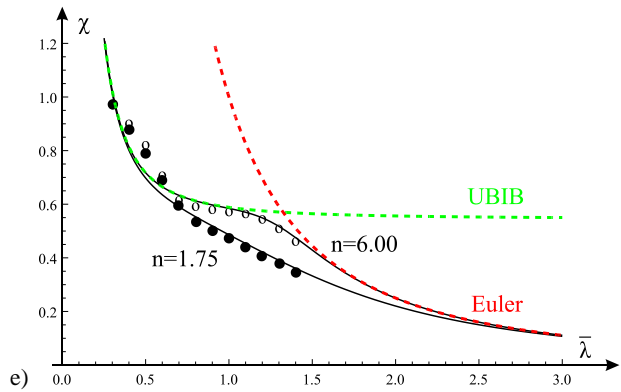
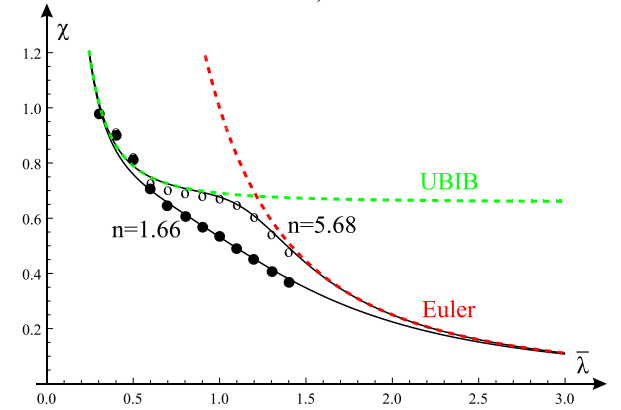
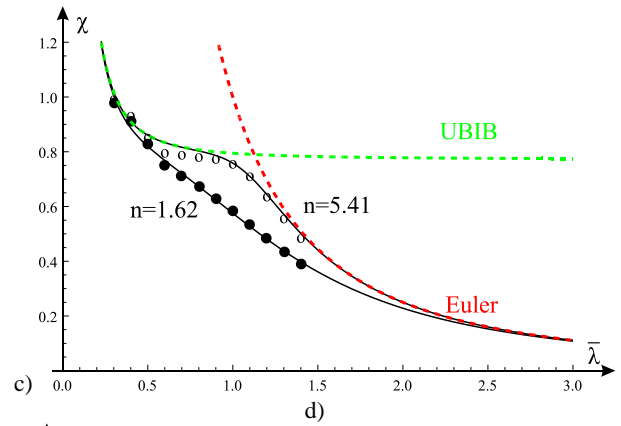
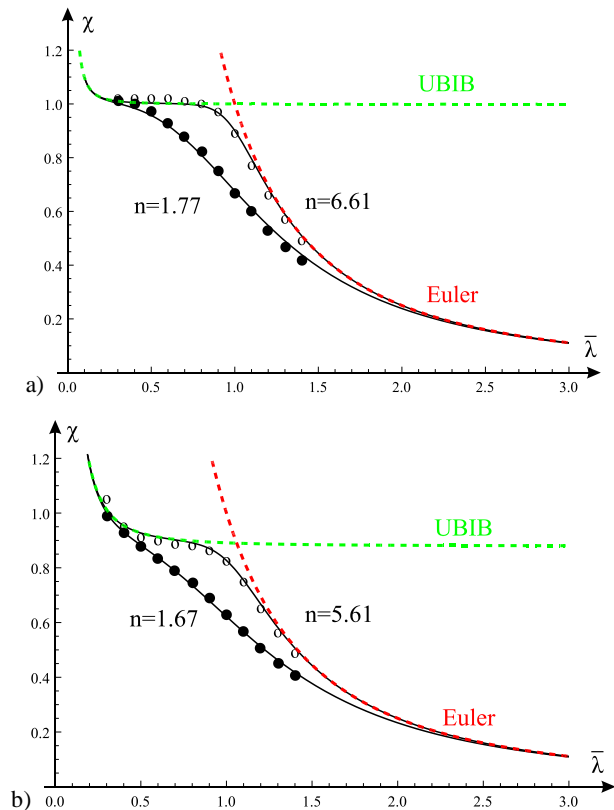


Fig. 7. Reduction factors χ_z calculated analytically and $\chi_{z,FEM}$ from FEM simulations for steel grade S355, a) $\psi_{com}=0$, b) $\psi_{com}=0.1$, c) $\psi_{com}=0.2$, d) $\psi_{com}=0.3$, e) $\psi_{com}=0.4$, f) $\psi_{com}=0.5$

The best fit imperfection factors n are calibrated using again the Mathematica function Non-Linear Model Fit for $\psi_{com}=0$ and five nonzero values of ψ_{com} (see Tab.

1), and two extreme values of the geometric amplitude e_0 , namely $L/10000$ (quasi straight column) and $L/750$ (the amplitude at the manufacturing tolerance level). The results are presented in Fig. 7.

Analyzing the optimization parameters n presented in the graphs shown in Fig. 5 one can conclude that for a geometric imperfection magnitude factor equal to $L/10000$ the power coefficient is close to the value of 6.0 while in case of imperfection magnitude $L/750$ it is close to 1.6. Thus, in the former case:

$$\chi_z = \left\{ \left(\bar{\lambda}_z^{-2} \right)^6 + \left[(1 - \xi_E)(1 - \psi) + \xi_E \bar{\lambda}_z^{-2} \right]^6 \right\}^{-1/6} \leq 1 \quad (18)$$

and in the latter:

$$\chi_z = \left\{ \left(\bar{\lambda}_z^{-2} \right)^{1.6} + \left[(1 - \xi_E)(1 - \psi) + \xi_E \bar{\lambda}_z^{-2} \right]^{1.6} \right\}^{-1/1.6} \leq 1 \quad (19)$$

in which for $\psi_{com} > 0$ the parameters $\xi_E = \xi_{E,eff}$ and $\psi = \psi_{eff}$ have to be taken from Tab. 1 for the BF model.

In Fig. 8, the buckling curves using the BF model approximations according to Eqns. (18) and (19) are presented for two extreme values of the geometric imperfection amplitude factor equal to $1/10000$ (upper curve) and $1/750$ (lower curve). Comparing the accuracy of buckling curves in Figs. 7 and 8 in reference to their discrete FEM results one can conclude that the buckling curves given in Fig. 8 are acceptable from engineering point of view. It is therefore justifiable to calibrate the imperfection factor n as a function of the geometric amplitude e_0 while the factor itself is to be independent from the effective stress strain parameters $\xi_E = \xi_{E,eff}$ and $\psi = \psi_{eff}$.

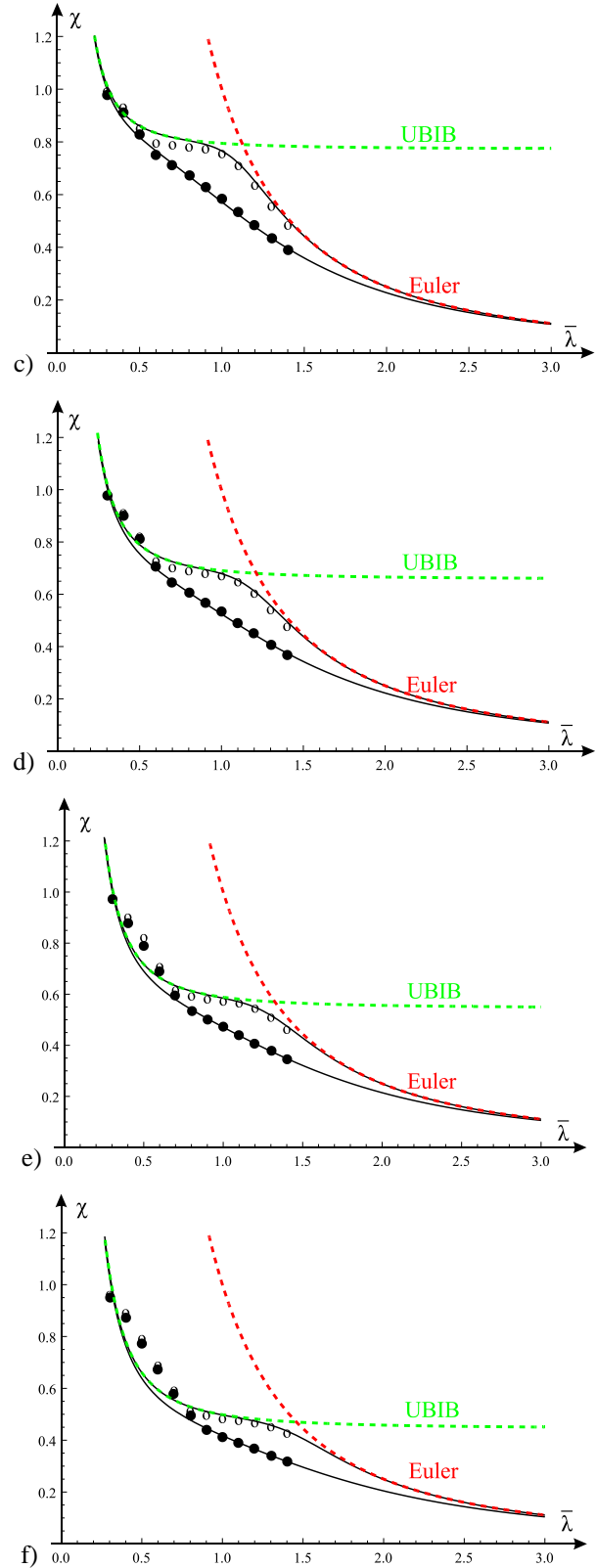
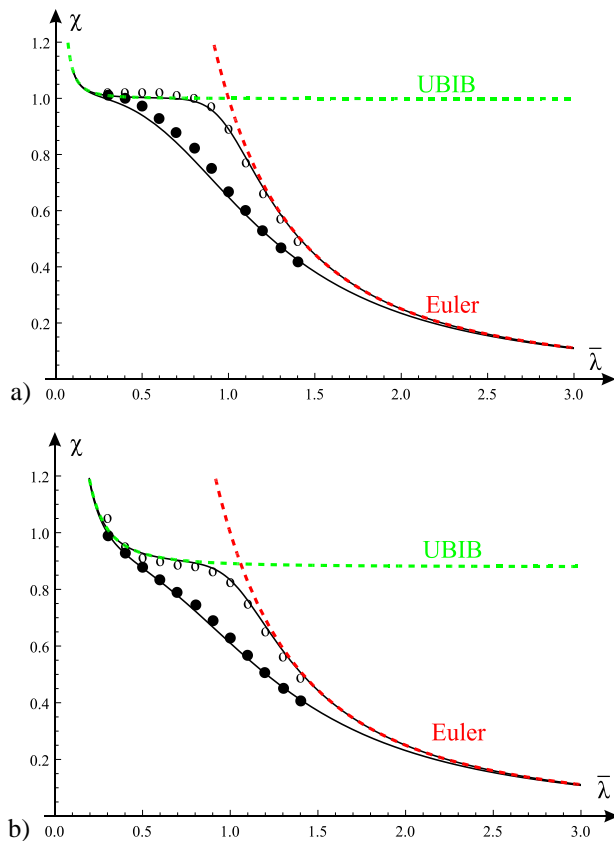


Fig. 8. Reduction factors χ_z calculated analytically for $n=6.0$ ($1/10000$) and $n=1.6$ ($1/750$), and $\chi_{z,FEM}$ from FEM simulations for steel grade S355, a) $\psi_{com}=0$, b) $\psi_{com}=0.1$, c) $\psi_{com}=0.2$, d) $\psi_{com}=0.3$, e) $\psi_{com}=0.4$, f) $\psi_{com}=0.5$

5 Conclusions

The paper deals with modelling of the residual postwelding stresses influence on the column overall

buckling. The analytical approach is presented on three different levels. First model (SE) based on strain free and internally equilibrated residual stresses gives acceptable predictions for slenderness $\bar{\lambda}_z$ above 0.6. In case of lower slenderness the numerical results are not in the domain indicated by this model. As a solution for this problem, the second formulation is applied (SC). This approach is based not only on analytical formulas, but for the determination of its parameters the virtual experiment on a stub element is needed. It is worth to underline here that the relationship for effective stresses and effective strains in tension range is different than those in compression. As a basis for SC parameters determination, the compression test is used. In that case, the prediction of the model is better than SE model, but still for low slenderness the numerical results lay outside the model domain. As a solution to these problem, the third model is applied, for which the model parameters are determined through nonlinear optimization methods. The model best fit parameters are then used for building up the M-R-M curves giving proper predictions for the whole range of geometrical imperfection multipliers. It is worth to indicate that BF model parameters work better for covering the effect of lower levels of residual stresses on the column buckling resistance. The biggest discrepancies are visible for slenderness below 0.6 and ψ_{com} within the range of 0.4-0.5. The buckling curve predictions for this range are however on a safe side.

References

1. L. Simoes da Silva, R. Simoes, H. Gervasio, *Design of Steel Structures (2nd Edition), Eurocode 3: Design of Steel Structures, Part 1-1: General Rules and Rules for Buildings, ECCS Eurocode Design Manual, Ernst & Sohn, Berlin (2016)*
2. EN-1993-1-1. Eurocode 3: Design of steel structures Part 1-1: General rules and rules for buildings, Brussels, European Committee for Standardization (2005)
3. J. Murzewski, *Reliability of engineering structures*. Arkady, Warszawa (1989) [in Polish]
4. A.M. Barszcz, M.A. Giżejowski, A generalized M-R-M approach for modelling of the stability behaviour of imperfect steel elements and structures, *Archives of Civil Engineering*, LII, **1**, 59-86 (2006)
5. R. Szczerba, M. Gajewski, M. Giżejowski, On modelling of the buckling resistance of welded I-section columns, II Baltic Conference for Students and Young Researchers BalCon2018 (2018) [in press]
6. M.A. Giżejowski, R. Szczerba, M.D. Gajewski, Z. Stachura: Buckling resistance assessment of steel I-section beam-columns not susceptible to LT-buckling. *Archives of Civil and Mechanical Engineering*, **17**, 2, 205-221 (2017)
7. *ABAQUS Theory manual*, Version 6.11, Dassault Systèmes (2011)
8. *ABAQUS/Standard User's manual*, Version 6.11, Dassault Systèmes (2011)
9. B. Launert, R. Szczerba, M. Gajewski, M. Rhode, H. Pasternak, M. Giżejowski, The buckling resistance of welded plate girders taking into account the influence of post-welding imperfections – Part 1: Parameter study, *Materials testing*, **59**, 1, 47-56 (2017)
10. B. Launert, M. Rhode, A. Kromm, H. Pasternak, T. Kannengiesser, Residual Stress Influence on the Flexural Buckling of Welded I-Girders, *Proceedings of International Conference on Residual Stresses*, Sydney, *Materials Research Proceedings*, **2**, 109-114 (2016)
11. B. Launert, H. Pasternak, Weld residual stresses effects in the design of welded plate girders: Simulation and Implementation, *Proceedings of Eurosteel 2017*, **1**, 2-3, 1039-1047 (2017)
12. N. Boissonnade, H. Somja, Influence of Imperfections in FEM Modeling of Lateral Torsional Buckling, *Proceedings of the Annual Stability Conference*, Structural Stability Research Council Grapevine (2012)
13. L. Simoes da Silva, L. Marques, C. Rebelo, Numerical validation of the general method in EC3-1-1 for prismatic members, *Journal of Constructional Steel Research*, **66**, 575-590 (2010)
14. F. Bijlaard, M. Feldmann, J. Naumes, G. Sedlacek, The “general method” for assessing the out-of-plane stability of structural members and frames and the comparison with alternative rules in EN 1993 – Eurocode 3 – Part 1-1, *Steel Construction*, **3**, 1, 19-33 (2010)
15. A. Agüero, L. Pallarés, F.J. Pallarés, Equivalent geometric imperfection definition in steel structures sensitive to flexural and/or torsional buckling due to compression, *Engineering Structures*, **96**, 160-177 (2015)
16. F. Papp, Buckling assessment of steel members through overall imperfection method. *Engineering Structures*, **106**, 124-136 (2016)
17. T. Tankova, L. Marques, L. Simões da Silva, A. Andrade, Development of a consistent methodology for the out-of-plane buckling resistance of prismatic beam-columns, *Journal of Constructional Steel Research*, **128**, 839-852 (2017)
18. Z. Kala, Sensitivity and reliability analyses of lateral-torsional buckling resistance of steel beams, *Archives of Civil and Mechanical Engineering*, **15**, 1098-1107 (2015)
19. Z. Kala, J. Valeš, Global sensitivity analysis of lateral-torsional buckling resistance based on finite element simulations, *Engineering Structures*, **134**, 37-47 (2017)
20. Z. Kala, J. Valeš, Sensitivity assessment and lateral-torsional buckling design of I-beams using solid finite elements, *Journal of Constructional Steel Research*, **139**, 110-122 (2017)